Journal of Applied Remote Sensing

Improving urban land use and land cover classification from high-spatial-resolution hyperspectral imagery using contextual information

He Yang
Ben Ma
Qian Du
Chenghai Yang

Improving urban land use and land cover classification from high-spatial-resolution hyperspectral imagery using contextual information

He Yang,[a] Ben Ma,[a] Qian Du,[a] and Chenghai Yang[b]
[a] Mississippi State University, Department of Electrical and Computer Engineering, Geosystems Research Institute, Mississippi State, Mississippi 39762
{hy58,bm538,du}@ece.msstate.edu
[b] United Stated Department of Agriculture, Agricultural Research Service, Kika de la Garza Subtropical Agricultural Research Center, Weslaco, Texas 78596
chenghai.yang@ars.usda.gov

Abstract. In this paper, we propose approaches to improve the pixel-based support vector machine (SVM) classification for urban land use and land cover (LULC) mapping from airborne hyperspectral imagery with high spatial resolution. Class spatial neighborhood relationship is used to correct the misclassified class pairs, such as roof and trail, road and roof. These classes may be difficult to be separated because they may have similar spectral signatures and their spatial features are not distinct enough to help their discrimination. In addition, misclassification incurred from within-class trivial spectral variation can be corrected by using pixel connectivity information in a local window so that spectrally homogeneous regions can be well preserved. Our experimental results demonstrate the efficiency of the proposed approaches in classification accuracy improvement. The overall performance is competitive to the object-based SVM classification.

Keywords: urban land use land cover mapping, hyperspectral imaging, support vector machine, pixel-based classification, object-based classification.

1 INTRODUCTION

As the most dynamic region on the earth, urban areas are of great interest to researchers and practitioners on planning and environmental management. The information on urban surface, such as land use and land cover (LULC) patterns, is critical to a range of themes in earth sciences including climatology, environmental change, and human-environment interactions. As remote sensing providing a synoptic overview for large regions, it becomes a very useful tool in urban monitoring [1].

In this paper, we will focus on LULC classification, which is often the basic step in more advanced applications. Many approaches have been developed to achieve classification, such as maximum likelihood classifier (MLC), neural-fuzzy method [2], etc. Recently, the support vector machine (SVM) becomes very popular, which is reported as one of the most powerful classifiers [3-5]. It is a supervised learning method, which constructs a hyperplane or set of hyperplanes in a high or infinite dimensional space where class separability is improved. In our research, we adopt SVM for LULC classification.

Hyperspectral imagery has been very useful for urban monitoring because its high spectral resolution provides more diagnostic power in detecting, classifying, and quantifying the materials on the earth than the traditional multispectral imagery with only several wide-band spectral channels [6]. Due to the advanced sensor technology, the spatial resolution of hyperspectral imagery is also greatly improved. Hyperspectral images with high spatial and spectral resolution can provide a large amount of detailed class information. Under this

Received 30 Mar 2010; accepted 4 Jun 2010; published 31 Aug 2010 [CCC: 19313195/2010/$25.00]

circumstance, both spatial and spectral information can be utilized to improve the accuracy of LULC classification [7-10].

One of the challenges of classifying a hyperspectral image is that the within-class spectral variation may lead to overall classification of spectrally homogeneous areas, resulting in salt-and-pepper noise in the classification map of these areas [11-12]. One way to alleviating the impact from trivial spectral variations is to employ object-based classification, where image segmentation is conducted first, followed by the classification of segmented objects [11-15]. Obviously, the key step in object-based classification is segmentation. The fractal net evolution approach (FNEA) [16], available in the eCognition software, is considered as a very successful approach in object segmentation. Basically, it treats image information as fractal, extracts the objects at a scale of interest based on fuzzy set theory, and combines the global and local mutual best fittings to generate image segments [17-18]. After segmentation, objects, as the basic processing units, can be classified using different methods, such as SVM [19].

In summary, we will investigate urban LULC classification from hyperspectral imagery with high spatial resolution using SVM in this paper. We will include class spatial information to correct the pixel-based SVM classification result in a post-processing step. The object-based classification, i.e., FNEA-based segmentation followed by SVM, will be used for comparison purpose. The experimental results will demonstrate that the proposed approaches will significantly improve classification accuracy.

2 METHODS

As mentioned earlier, spatial information can be used to improve classification accuracy when dealing with a hyperspectral image with high spatial resolution. The frequently used spatial features include texture, class shape, and size. There features are concrete and can be extracted directly from raw data, which are called "low-level" spatial features in this paper. On the contrary, "high-level" spatial features are more abstract and defined based on human understanding, such as class neighborhood relationships, the correlation between a certain class presence and geographical location. In some cases, it may be still difficult to separate different classes based on low-level spatial features. For instance, it is usually necessary to classify road, grass, tree, trails, shadow, water, and roof in an urban area. The initial classification result may include some misclassified pairs, such as roof-road and trail-roof, because their spectral features are similar and extracted spatial features such as texture are not effective in separating them from each other. Thus, in this paper, we propose to use high-level spatial information including class neighborhood relationship to correct misclassified class pairs. To further remove salt-and-pepper noise for any class in a homogeneous area, we also propose a simple filtering method based pixel connectivity.

The overall classification diagram is shown in Fig. 1, where a two-stage correction procedure is deployed on the SVM result. For SVM classification, principal component analysis (PCA) is used for dimensionality reduction and the first several principal components (PCs) actually participate in classification. Here, the number of PCs chosen is equal to the number of classes. In general, using dimensionality-reduced data, SVM can provide better performance. The radial basis function (RBF) kernel is employed for the SVM classifier.

Fig.1. The overall classification diagram.

2.1 Correction based on class neighborhood relationship

In general, an urban area is well designed and organized, and this hidden nature is the high-level spatial information which can be utilized to improve classification accuracy. One kind of information is about the neighborhood relationship among different classes. Even when their low-level feature vectors (i.e., texture-based features) are similar, the high-level features "embedded" in their class neighborhood relationship may provide some "error-correction" capability. Here we focus on two class pairs prone to be misclassified, i.e., trail-roof and roof-road. In the urban environment, a trail is usually built among trees and grass; although it may be close to a building (roof), a trail pixel should have more other trail pixels than roof pixels as its immediate neighbors. Such information is presented in Fig. 2 as possible patterns for a trail pixel centered in a 3 × 3 window. Thus, for the trail-roof pair, we may have the following rule for correction.

1) When the central pixel in a local window is pre-classified as trail pixel:
- Pattern 1: A trail pixel has one or more grass or tree pixels as neighbors.
- Pattern 2: A trail pixel has more trail neighbors than non-trails neighbors.
- Roof-trail error pattern: If not belonging to the above two patterns, the pixel is most likely a roof pixel rather than a trail pixel.

2) When the central pixel is pre-classified as roof pixel:
- Trail-roof error pattern: If it has grass/tree neighboring pixels and has more trail neighbors than roof neighbors, the pixel is most likely a trail pixel rather than a roof pixel.

For the roof-road pair, the situation is more complicated due to the fact that their neighbors are highly variable and can be quite similar. Therefore, as shown in Fig. 2, the correction is simply based on the majority rule.

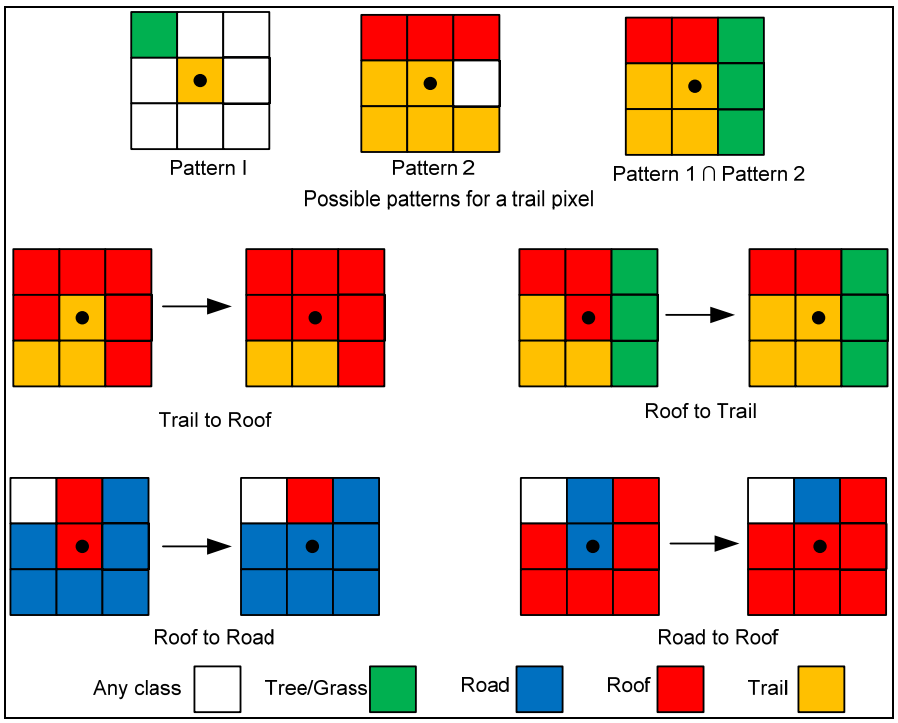

Fig.2. The proposed correction schemes for the pairs of trail-roof and roof-road.

```
Input: SVM-based classification map
do (in a sliding window)
    if (central pixel is trail) and (not (pattern I or pattern II))
     change central pixel to roof
    if (central pixel is roof) and (trail-roof error pattern )
     change central pixel to trail
while (number of changed pixels > 0)
do
    if (central pixel is roof) and (roof neighbor < 2 and road neighbor > 5)
    change central pixel to road
    if (central pixel is road) and (road neighbor < 2 and roof neighbor > 5)
    change central pixel to roof
while (number of changed pixels > 0)
```

Fig. 3. Pseudocode for the class neighborhood-based correction algorithm.

The pseudocode for the correction algorithm based on class neighborhood relationship is summarized in Fig. 3, where the classes prone to be misclassified are assumed to be the pairs of trail- roof and roof- road. Several points are noteworthy.

- The correction procedure will automatically start from the boundary of each class, and gradually move to the inner part. This is because boundary pixels are prone to be misclassified and newly corrected pixels will provide new spatial information which can be used in the following correction process.
- The correction procedure should be done one class after another. This is because the previously corrected pixels may be critical in correcting the misclassified pixels in other classes. The procedure should start from a class that does not rely on the correction results from other classes.
- For different classes, the chance for their misclassified pixels to be corrected is different. For instance, the neighbor of a tree pixel or a grass pixel is highly variable, so it is very difficult to correct a misclassified tree or grass pixel based on class neighborhood information. Hence, other correction rule, such as the one based on pixel connectivity, is proposed.

2.2 Correction based on connectivity

To remove the effect of salt-and-pepper noise in a classification map, a post-filter such as morphological filter, can be applied. Here, we propose a simpler method based on connectivity for this purpose. For a given 3×3 window, the connectivity of the central pixel's neighboring pixels is analyzed. Instead of counting the number of pixels belonging to the same class in the eight neighboring pixel, we count the number of pixels belonging to the same class and the same connected component. If the number exceeds a threshold, the center pixel is reclassified to the class of this connected component. In this way, the isolated salt-and-pepper noise in a classified homogeneous area can be further reduced. As illustrated in Fig. 4(b), there are four connected regions: region I, region II, region III, and region IV. Although there are four pixels belonging to the same class represented in red color, these four pixels are separated into region I and region III. Then we count the number of connected pixels in each region: 2 pixels in region I, 1 in region II, 2 in region III, and 3 in region IV. The maximum number is 3, which is for the class in blue, so the central pixel is reclassified into the class in blue.

The corresponding pseudocode is shown in Fig. 5. Note that this correction is for any class, not limited to trail- roof and roof- road pairs as discussed in Section 2.1.

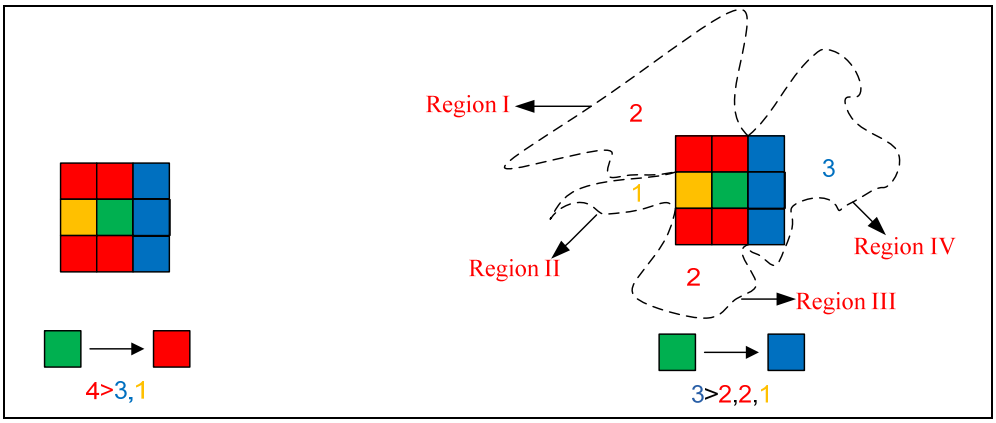

(a) without considering connectivity (b) with considering connectivity

Fig.4. Illustration of the connectivity-based correction.

Input: SVM-based classification map after the class neighborhood-based correction.
do: Generate the connected component label for each class
for a center pixel in a local window
count the number of its neighboring pixels in the same connected component
if (this number is greater than the threshold)
then set the central pixel's class label to that of the most connected neighboring pixels
end

Fig.5. Pseudocode for the connectivity-based correction algorithm.

3 RESULTS

3.1 HYDICE data experiment I

The hyperspectral data used in the experiments was taken by the airborne Hyperspectral Digital Imagery Collection Experiment (HYDICE) sensor. It was collected for the Mall in Washington, DC with 210 bands covering 0.4-2.4 μm spectral region. The spatial resolution is about 2.8m. The low signal-to-noise ratio (SNR) and water-absorption bands were deleted, resulting in 191 bands. The original data has 1280 × 307 pixels. The original image was cropped into a subimage of size 304 × 301 pixels. The image in pseudocolor was shown in Fig. 6, which includes six classes: {road, grass, shadow, trail, tree, roof}. From Fig. 6, we can see that roof areas exhibit obviously different spectral signatures. The number of samples for each class was listed in Table 1 with total 309 training samples and 4772 test samples.

The classification map from SVM was shown in Fig. 7(a), where many roof areas (displayed in orange) were classified as trail (displayed in yellow). There were also some misclassification between roof and road. The classification map after the proposed two-stage correction was shown in Fig. 7(b), where the misclassified roof areas were corrected, showing

larger areas in orange. The road class in gray was also cleaned up. Table 2 listed the classification accuracy of each class and the overall accuracy (OA) and average accuracy (AA) for SVM before correction, SVM after correction, and FNEA segmentation followed by SVM. From Table 2, we can see that the improvement on roof classification was significant. The OA value was increased from 93.6% to 97.4% after correction, and AA value from 94.0% to 97.2%. The object-based classification provided a little lower OA and AA than the original SVM.

Fig. 6. The image scene used in HYDICE experiment 1.

Table 1. Training and test samples used in HYDICE experiment 1.

	Training	**Test**
Road	55	892
Grass	57	910
Trail	50	567
Tree	46	624
Shadow	49	656
Roof	52	1123
Total	**309**	**4772**

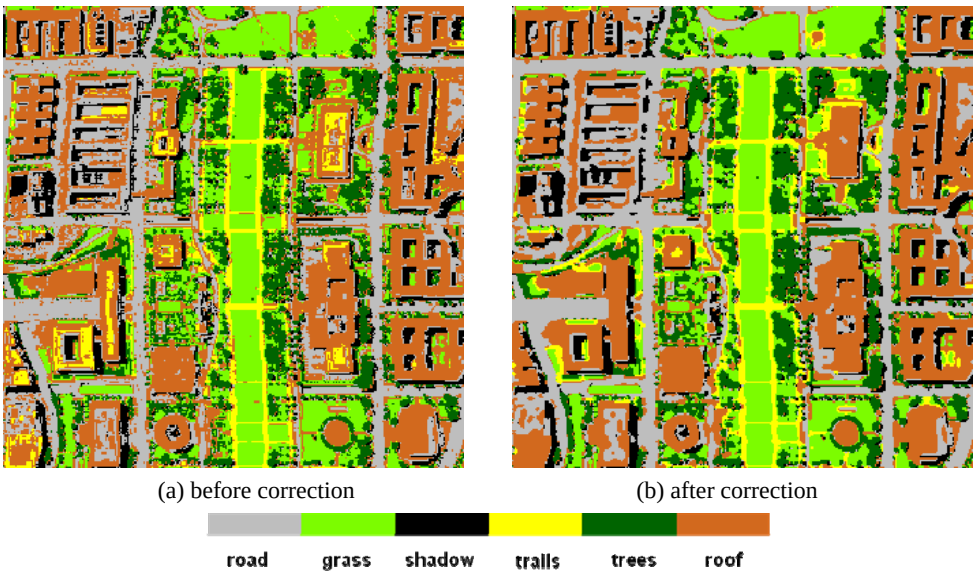

(a) before correction (b) after correction

Fig. 7. Classification map using SVM for Fig. 6.

Table 2. Classification accuracy from different methods in HYDICE experiment 1.

	SVM (before correction)	SVM (after correction)	FNEA
Road	96.4%	99.6%	95.2%
Grass	97.3%	97.3%	86.7%
Shadow	88.2%	91.4%	97.4%
Trail	97.0%	98.1%	88.0%
Tree	98.9%	99.4%	86.1%
Roof	86.3%	97.5%	89.7%
OA	93.6%	97.4%	89.6%
AA	94.0%	97.2%	90.5%

3.2 HYDICE data experiment II

The HYDICE Washington DC Mall image was cropped into a small subimage with 266 × 304 pixels as shown in Fig. 8 in pseduocolor. It includes seven classes: {road, grass, water, shadow, trail, tree, roof}. Again, the spectral difference within the roof class was obvious. In addition, due to low spectral reflectance, water body and shadow classes may be difficult to be separated; they may not have concrete spatial features, making their separation more difficult. The number of training and test samples in each class was tabulated in Table 3.

The classification map from SVM was shown in Fig. 9(a), where many roof areas (in orange) were misclassified as trail (in yellow). The classification map after the proposed two-stage correction was shown in Fig. 9(b), where the misclassified roof areas were successfully corrected and displayed in larger orange regions. Meanwhile, road classification was also improved, resulting in less orange spots in the gray regions. Table 3 listed the classification accuracy of the three SVM-based approaches. From Table 3, we can see that the improvement on roof classification was significant, while the classification accuracy of grass, tree, shadow, and water classes were almost intact due to the difficulty of further improvement. The OA

value was increased from 87.9% to 97.4% after correction, and AA value from 90.2% to 96.1%. In this experiment, the object-based classification provided similar accuracy as the original SVM.

Fig. 8. The image scene used in HYDICE experiment 2.

Table 3. Training and test samples used in HYDICE experiment 2.

	Training	**Test**
Road	63	1090
Grass	62	1082
Water	59	403
Trail	59	469
Tree	60	734
Shadow	61	461
Roof	60	1292
Total	**424**	**5531**

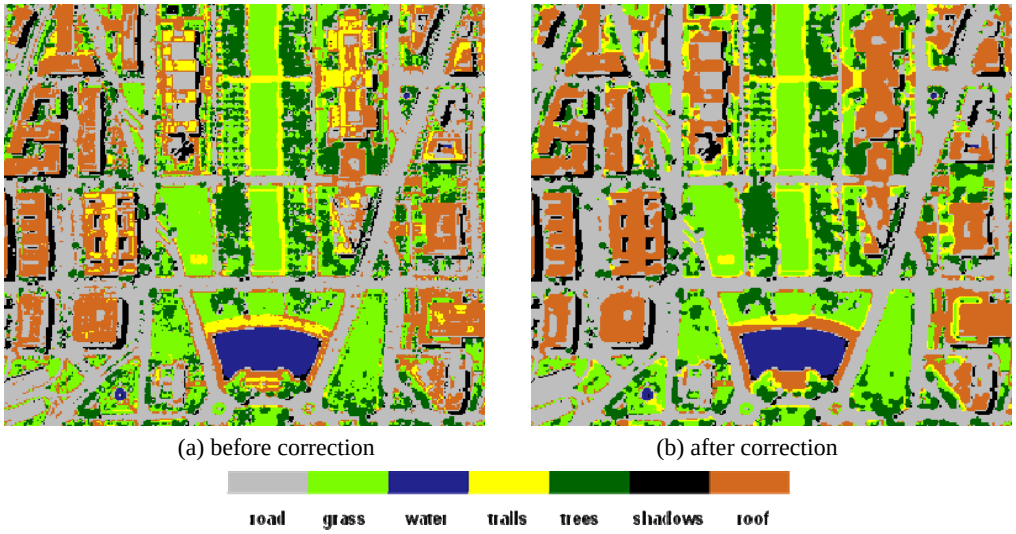

(a) before correction (b) after correction

Fig. 9. Classification map using SVM for Fig. 8.

Table 4. Classification accuracy from different methods in HYDICE experiment 2.

	SVM (before correction)	SVM (after correction)	FNEA
Road	98.8%	100.0%	94.6%
Grass	99.8%	100.0%	100%
Water	87.6%	87.4%	88.3%
Trail	99.7%	100.0%	73.2%
Tree	99.0%	99.3%	99.9%
Shadow	87.6%	87.4%	84.6%
Roof	58.9%	98.3%	79.6%
OA	87.9%	97.4%	87.6%
AA	90.2%	96.1%	88.6%

3.3 HyMap data experiment

Fig. 10 shows a 126-band HyMap data about a residential area near the campus of Purdue University. The image size is 377 × 512. The spatial resolution is 3.5m. The image scene includes six classes: {road, grass, shadow, soil, tree, roof}. As listed in Table 5, 404 training samples and 5463 test samples were available. Compared to the previous two experiments, roof class in this image was more spectrally homogeneous. Instead, the road class seemed to have within-class spectral variation; it also had different spatial shapes in different areas, which made it difficult to employ an effective "low-level" spatial feature.

The classification map from SVM was shown in Fig. 11(a), where the majority of misclassifications happened within the road-soil pair due to the spectral similarity between soil and road paving materials. The correction rule for road-trail in the previous two experiments was employed here. The classification map after the proposed two-stage correction was shown in Fig. 11(b), where larger and smoother homogeneous areas were displayed. For instance, the road regions in gray had less spot noise after correction; the tree regions in dark green were more homogeneous. Table 6 listed the classification accuracy of the three SVM-based approaches, where the improvement on road, soil, tree, and grass classification was significant. Both values of OA and AA were approximately improved by 2% using the two-stage correction. The FNEA provided slightly less accurate result than the original SVM.

Fig. 10. The image scene used in HyMap experiment.

Table 5. Training and test samples used in HyMap experiment.

	Training	**Test**
Road	73	1231
Grass	72	1072
Shadow	49	215
Soil	69	380
Tree	67	1321
Roof	74	1244
Total	**404**	**5463**

(a) before correction

(b) after correction

Fig. 11. Classification map using SVM for Fig. 10.

Table 6. Classification accuracy from different methods in HyMap experiment.

	SVM (before correction)	SVM (after correction)	FNEA
Road	93.6%	97.2%	87.5%
Grass	98.9%	99.9%	96.5%
Shadow	97.2%	97.2%	80.0%
Soil	91.1%	94.6%	87.7%
Tree	96.6%	99.0%	97.3%
Roof	81.3%	82.2%	84.7%
OA	92.5%	94.6%	90.6%
AA	93.1%	95.0%	89.0%

4 CONCLUSION

In this paper, we propose approaches to improve the pixel-based SVM classification using class spatial neighborhood relationship and pixel connectivity. The class spatial neighborhood relationship can help correct the misclassified class pairs, such as roof and trail, road and roof. These classes may be difficult to be separated because they may have similar spectral signatures and their spatial features are not distinct enough. Based on pixel connectivity, misclassification incurred from within-class trivial spectral variation can be corrected so that spectrally homogeneous regions can be well preserved. Our experimental results demonstrate the efficiency of the proposed approaches in classification accuracy improvement. The overall performance is competitive to the object-based SVM classification.

To ensure classification improvement using the proposed approaches, it is required to have a deep understanding about the image scene and different class patterns in order to abstract the useful high-level spatial relationship for correction.

Acknowledgments

The authors would like to thank Dr. David Landgrebe at Purdue University for providing the data used in the experiments. The authors also thank Drs. Liangpei Zhang and Xin Huang at Wuhan University for providing the ground truth data and object-based classification results for comparison.

References

[1] Q. Weng and D. A. Quattrochi, *Urban Remote Sensing*, CRC Press, Boca Raton, FL (2006).

[2] H.-W. Chen, N.-B. Chang, R.-F. Yu, and Y.-W. Huang, "Urban land use and land cover classification using neural-fuzzy inference approach with Formosat-2 data," *J. Appl. Remote Sens.* **3**, 033558 (2009) [doi:10.1117/1.3265995].

[3] R. E. Karlsen, D. J. Gorsich, and G. R. Gerhart, "Target classification via support vector machine," *Opt. Eng.* **39**, 704-711 (2000) [doi:10.1117/1.602417].

[4] G. Zhu and D. G. Blumberg, "Classification using ASTER data and SVM algorithms: The case study of Beer Sheva, Israel," *Remote Sens. Environ.* **80**, 233-240 (2002) [doi:10.1016/S0034-4257(01)00305-4].

[5] S. van der Linden, A. Janz, B. Waske, M. Eiden, and P. Hostert, "Classifying segmented hyperspectral data from a heterogeneous urban environment using support vector machines," *J. Appl. Remote Sens.* **1**, 013543 (2007) [doi:10.1117/1.2813466].

[6] R. V. Platt and A. F. H. Goetz, "A Comparison of AVIRIS and Landsat for land use classification at the urban fringe," *Photogram. Eng. Remote Sens.* **70**, 813-819 (2004).
[7] F. Dell' Acqua, P. Gamba, A. Ferari, J. A. Palmason, J. A. Benediktsson, and K. Arnason, "Exploiting spectral and spatial information in hyperspectral urban data with high resolution," *IEEE Geosci. Remote Sens. Lett.* **1**, 322-326 (2004) [doi:10.1109/LGRS.2004.837009].
[8] J. A. Benediktsson, J. A. Palmason, and J. R. Sveinsson, "Classification of hyperspectral data from urban areas based on extended morphological profiles," *IEEE Trans. Geosci. Remote Sens.* **43**, 480-491 (2005) [doi:10.1109/TGRS.2004.842478].
[9] J. Stuckens, P. R. Coppin, and M. E. Bauer, "Integrating contextual information with per-pixel classification for improved land cover classification," *Remote Sens. Environ.* **71**, 282-296 (2000) [doi:10.1016/S0034-4257(99)00083-8].
[10] T. Kasetkasem, M. K. Arora, and P. K. Varshney, "Super-resolution land cover mapping using a Markov random field based approach," *Remote Sens. Environ.* **96**, 302-314 (2005) [doi:10.1016/j.rse.2005.02.006].
[11] B. Zhang, X. Jia, Z. Chen, and Q. Tong, "A patch-based image classification by integrating hyperspectral data with GIS," *Int. J. Remote Sens.* **27**, 3337-3346 (2006) [doi:10.1080/01431160500409577].
[12] X. Huang and L. Zhang, "Object-oriented subspace analysis for airborne hyperspectral remote sensing imagery," *Neurocomput.* **73**, 927-936 (2010) [doi:10.1016/j.neucom.2009.09.011].
[13] R. L. Kettig and D. A. Landgrebe, "Classification of multispectral image data by extraction and classification of homogeneous objects," *IEEE Trans. Geosci. Electron.* **GE-14**, 19-26 (1976) [doi:10.1109/TGE.1976.294460].
[14] X. Huang and L. Zhang, "An adaptive mean-shift analysis approach for object extraction and classification from urban hyperspectral imagery," *IEEE Trans. Geosci. Remote Sens.* **46**, 4173-4185 (2008) [doi:10.1109/TGRS.2008.2002577].
[15] D. Forster, Y. Buehler, and T. W. Kellenberger, "Mapping urban and peri-urban agriculture using high spatial resolution satellite data," *J. Appl. Remote Sens.* **3**, 033523 (2009) [doi:10.1117/1.3122364].
[16] *eCognition Professional User Guide 4*, Munich, Germany, (2003), http://www.definiens-imaging.com
[17] M. Baatz and A. Schäpe, "Multiresolution segmentation - an optimization approach for high quality multi-scale image segmentation," (2000), http://www.ecognition.com/document/multiresolution-segmentation-optimization-approach-high-quality-multi-scale-image-segmentat
[18] G. J. Hay, T. Blaschke, D. J. Marceau, and A. Bouchard, "A comparison of three image-object methods for the multiscale analysis of landscape structure," *ISPRS J. Photogram. Remote Sens.* **57**, 327-345 (2003) [doi:10.1016/S0924-2716(02)00162-4].
[19] L. Bruzzone and L. Carlin, "A multilevel context-based system for classification of very high spatial resolution images," *IEEE Trans. Geosci. Remote Sens.***44**, 2587-2600 (2006) [doi:10.1109/TGRS.2006.875360].

He Yang received his B. S. degree in Communication Engineering from University of Electronic Science and Technology of China in 2004. He is currently pursuing Ph. D. degree in the Department of Electrical and Computer Engineering at Mississippi State University. His research interests include hyperspectral image analysis and parallel computing.

Ben Ma received his B. S. degree in electrical engineering from Northwestern Polytechnical University, Xi'an, China, in 2007. He is currently pursuing Ph. D. degree in the Department of Electrical and Computer Engineering at Mississippi State University. His research interests include hyperspectral image analysis, pattern recognition, and video processing.

Qian Du received her Ph.D. degree in electrical engineering from University of Maryland Baltimore County in 2000. She currently is an Associate Professor in the Department of Electrical and Computer Engineering at Mississippi State University. Her research interests include remote-sensing image analysis, pattern classification, data compression, and neural networks.

Chenghai Yang is an agricultural engineer with the USDA Agricultural Research Service's Kika de la Garza Subtropical Agricultural Research Center at Weslaco, Texas. He received his B.S. and M.S. degrees in agricultural engineering from Northwest Agricultural University in China, and his Ph.D. degree in agricultural engineering from the University of Idaho. He has authored or coauthored numerous journal articles and other technical publications on remote sensing applications. His current research is focused on the use of remote sensing and other spatial information technologies for mapping invasive weeds in rangeland and wetland ecosystems and for mapping crop yield and growth conditions for precision agriculture.